NASA SP-5965 (01)
January 1976

TECHNOLOGY UTILIZATION

OPTICAL DEVICES

A COMPILATION

NATIONAL AERONAUTICS AND SPACE ADMINISTRATION

Foreword

The National Aeronautics and Space Administration has established a Technology Utilization Program for the dissemination of information on technological developments which have potential utility outside the aerospace community. By encouraging multiple application of the results of its research and development, NASA earns for the public an increased return on the investment in aerospace research and development programs.

This Compilation is part of a series intended to provide such technical information. The items reported range widely in the field of optics and optical devices; they may interest scientists, engineers, and technicians.

Additional technical information on individual devices and techniques can be requested by circling the appropriate number on the Reader Service Card included in this Compilation.

The latest patent information available at the final preparation of this Compilation is presented on the page following the last article in the text. For those innovations on which NASA has decided not to apply for a patent, a Patent Statement is not included. Potential users of items described herein should consult the cognizant organization for updated patent information at that time.

We appreciate comment by readers and welcome hearing about the relevance and utility of the information in this Compilation.

Technology Utilization Office
National Aeronautics and Space Administration

For sale by the National Technical Information Service, Springfield, Virginia 22161

Contents

Section 1. Optical Instrumentation

CALCULATIONS FOR ULTRAVIOLET REGION TELESCOPE DESIGN PARAMETERS

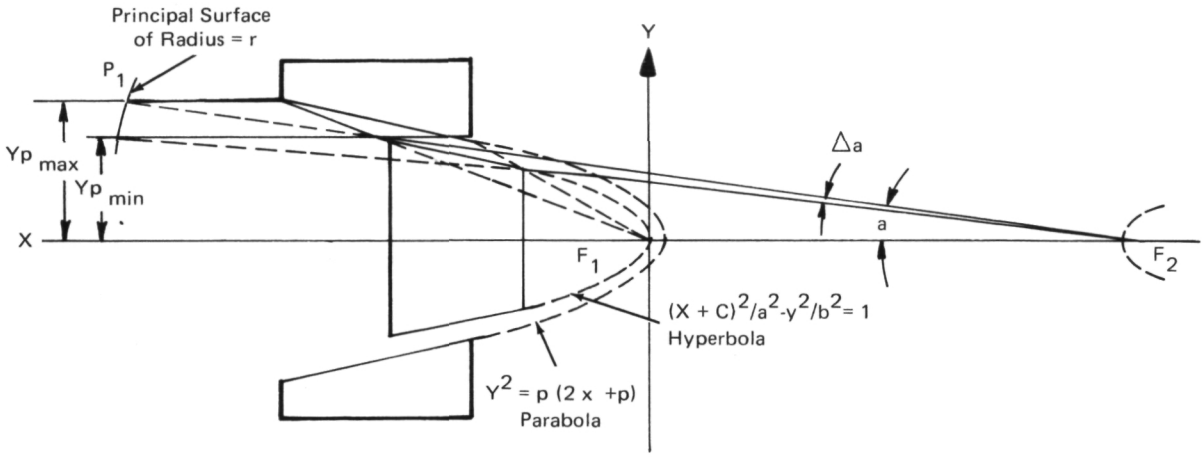

A procedure has been developed that solves the problem of selecting design parameters for a far-ultraviolet telescope for space applications when physical size must be minimized, optical acceptance (throughput) maximized, and high spatial (resolving power) and spectral (optical efficiency) properties realized. The technique evolved as a result of the need for an extreme ultraviolet image telescope for operation within constrained spaceflight conditions.

The basic design for a Type 2, or far-ultraviolet telescope, as shown in the figure, consists of surfaces of revolution. Except for the extreme obliqueness of the imaging surfaces, the geometry is identical to the Cassegrainian telescope. Incoming rays reflected by the paraboloid toward focus F_1 are in turn reflected to a conjugate focus F_2 by a confocal convex hyperboloid. The outer and inner edges of the paraboloid, $Y_{p\ max}$ and $Y_{p\ min}$, respectively, define the annular collecting area A of the telescope.

The principal surface conforms to a parabolic geometry defined by the equation

$$r = \left[\frac{pb^2}{2(c-a)^2} \quad (1 + \tan \alpha/2) \right] \qquad (1)$$

where r is the radius of the principal surface at angle α. Deviation of this surface from a spherical form for the Type 2 (as well as Type 1) telescope is given by

$$\Delta r = r(\Delta \alpha) \tan(\alpha_{max}\ 2) \qquad (2)$$

for rays which enter the system parallel to the optical axis. Since Δr may be considered as a measure of the offense against the sine condition (OSC), and therefore an indicator of optical performance, it is convenient to rewrite Equation (2) as a function of the design parameters of the telescope. To accomplish this, the folding ratio k is defined as the ratio of the physical length L to the effective focal length (f = r) of a telescope with a throughput (optical acceptance) of $\Omega = A\ r^2$. Equation (2) may now be expressed in terms of the design parameters by

$$\Delta r = (A/2\ \pi\ Y_{p\ max}) \tan(\alpha_{max}/2) \qquad (3)$$

or

$$\Delta r = \Omega L/2\ \pi k (1 + \cos \alpha_{max}), \qquad (4)$$

where the angle α_{max} is related to the effective focal ratio, f/#, of the telescope by the expression

$$\alpha_{max} = \sin^{-1} \left[1/2\ (f/\#) \ . \right] \qquad (5)$$

Source: J. D. Mangus
Goddard Space Flight Center
(GSC-11233)

Circle 1 on Reader Service Card.

MODIFICATIONS TO OPTICAL-DRILLING MICROSCOPES

Problems that may be encountered when using drilling microscopes, e.g., those used for working on printed circuit boards, are: the image may not be concentric with the background reticle, the image may be too small, or the image may be washed out by incident light on the viewing lens. A solution to these problems can be accomplished by making the following modifications: (1) replace the original mirror with a 1/2 surface mirror located on the optical axis of the viewing lens to center the image, (2) add a magnifying lens behind the viewing lens to enlarge the image, (3) attach an extended hood over the magnifying lens, and (4) coat all lenses to brighten the image.

The original mirror was located below the axis of the viewing lens to avoid obstruction of the image and reticle from the viewer. However, the angle between the axis of the reflected image and the viewing axis resulted in a vertically elongated image. A circular pattern placed beneath the objective lens appeared as an ellipse at the viewing lens. The problem of obstructed view was solved by the use of a transparent, 1/2 surface mirror (beam splitter). Moved upward, and centered on the viewing axis, this mirror supplies an undistorted image that is concentric with the circular reticle. A convex magnifying lens placed over the viewing lens produces the desired increase in image size without reducing the field of view. A cylindrical metal hood, grooved and blackened on its inside surface to suppress reflections, reduces incident light on the surface of the magnifier. Optical coating on all lenses further reduces reflection in the lens system. The result is a sharper and brighter image.

Source: A. J. Walch, Jr.
Goddard Space Flight Center
(GSC-09952)

No further documentation is available.

REDUCED DIAMETER TELESCOPE FOR REMOTE ACCESS INSPECTION

A reduced diameter tubular telescope has been proposed for use in mechanical inspection of obstructed areas in critical structures. The concept involves replacing the outer metal casting with a polyimide shell, thereby permitting the diameter of the telescope to be reduced from 2.67 mm to 2.03 mm.

In the design of access ports into obstructed areas of critical structures, to permit remote viewing for service inspection, it is important that the diameter of the ports required should be as small as possible. Currently, the smallest available tubular telescopes of 15.1 to 20.3 cm lengths are 2.67 mm in diameter. Smaller diameter inspection ports into these obstructed areas will be possible by reducing the diameter of the smallest available telescope incorporating a concentric fiber optic light input bundle.

To accomplish the necessary reduction, the metal outer wall is removed, the internal components are cast in a plastic matrix, and the sides are covered with a polyimide coating.

Source: W. McMahon of
Rockwell International Corp.
under contract to
Johnson Space Center
(MSC-17585)

No further documentation is available.

ELECTRONIC OPTICAL TRANSFER FUNCTION ANALYZER

Optical transfer function analyzers are devices for quantizing the resolving quality of an optical system. The measurement is analogous to using a bar chart without the subjectivity of the observer. The optical transfer function analyzer measures the light scattered out of a bright beam into an area which should be unlighted. If E(x) is the illumination on the face of the detector as a function of position x, the optical transfer function is found by taking the Fourier sine-cosine transform pair of the derivative of E(x). This can be performed numerically in the minicomputer. The computer sends out a digital signal to a digital-to-analog (D/A) converter which drives positioning coils. Thus, the computer determines the position x of the element on the face of the tube which is being monitored. The intensity of light on this element determines the number of electrons which go through the aperture in the image dissector and are amplified by the electron multiplier section of the image dissector. This amplified signal is fed to the analog-to-digital (A/D) converter which inputs the value E to the digital minicomputer. The computer now determines the position x_i, and measures the intensity, E, at x_i and thereby acquires the value $E(x_i)$. The computer now steps the beam so that point x_i is monitored. By continuing in this fashion every point x on the face of the tube can be monitored and the value of the function E(x) determined by the computer. A computer program which calculates the optical transfer function is then performed and the result is an output to any of a variety of output display devices, such as teletype, digital printer, CRT, or plotter.

The optical transfer function analyzer has no moving parts; there is no need for precision machine work of mechanical parts or for precision electric motors to scan a razor edge. Repeated scans can be performed with ease for averaging purposes of increasing the signal-to-noise ratio. The analyzer is faster, cheaper, more accurate, and does not require further computing equipment, as do current devices. The light source, collimator, optical bench and accessories required by the device are identical to those required by current devices.

Source: E. E. Klingman
Marshall Space Flight Center
(MFS-21672)

Circle 2 on Reader Service Card.

PRECISION MECHANICAL DRIVE IMPROVES SPECTRA-WIDENING MECHANISM: A CONCEPT

A mechanical spectra-widening mechanism costs one-fifth as much as current systems using electric motors with electronic controls and it provides a significant increase in reliability. A combination chain and gear drive tilts a spectrograph over a range of 270 arc-seconds with respect to an articulated mirror system, widening the spectra lines to approximately one millimeter and controlling spacing within 30 micrometers.

The unit consists primarily of a constant torque spring motor and a mechanical speed controller system. The constant torque motor can be energized by a hand crank. The output shaft is controlled by a uni-directional clutch and is connected to the speed controller through a gear train. The speed controller is essentially a centrifugal brake capable of controlling its output shaft for the required rpm. The output shaft drives a selectable speed type gear train. This output shaft rotation is transmitted through a reversible bevel gear set which in turn drives a worm gear assembly controlling motion within 30 micrometers of arc.

Source: S. Hornyak of
Martin Marietta Corp.
under contract to
Johnson Space Center
(MSC-13937)

Circle 3 on Reader Service Card.

A COMPLETE SYSTEM FOR RITCHEY-CHRETIEN TELESCOPE DESIGN

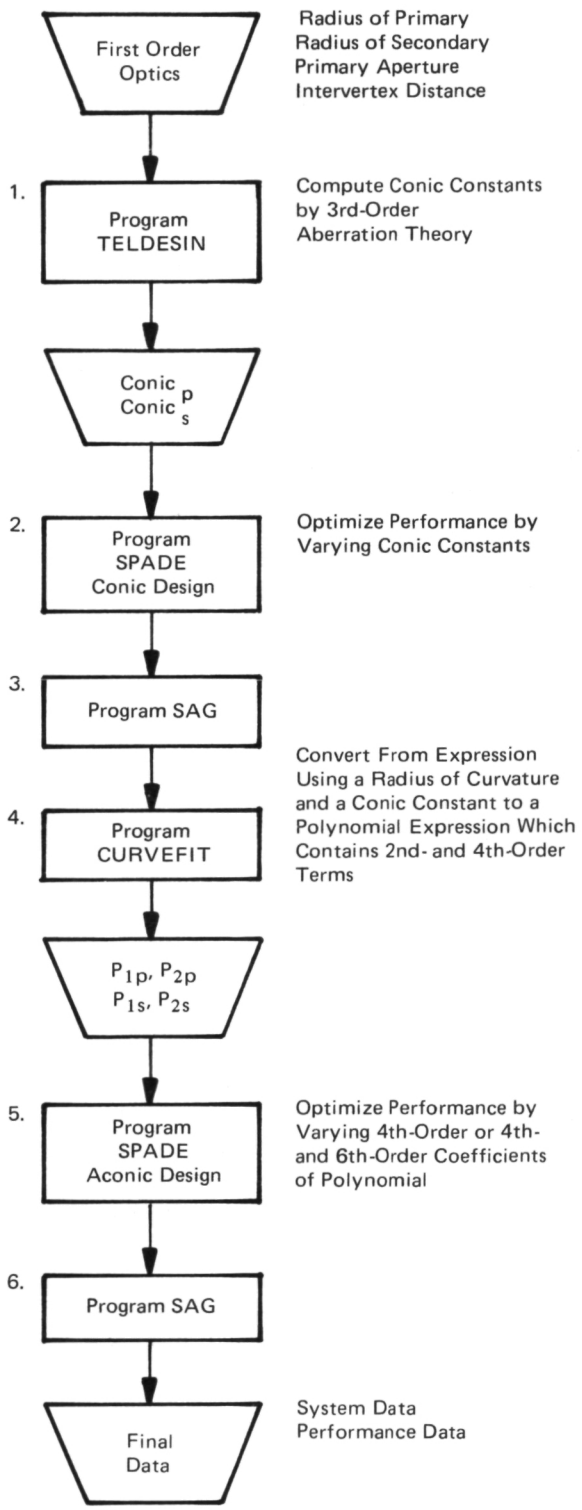

Flow Chart

In the design of two-mirror telescope systems for operation in either the ultraviolet or infrared region of the spectrum, it is often required that the telescope design be diffraction-limited in performance over a substantial field of view. The problem is to determine just what geometrical form the primary and secondary mirrors should have to achieve the desired performance.

There are various classes of telescope design to solve the two-mirror problem, among which are the Cassegrainian, the Dall-Kirkham, and the Ritchey-Chretien. The latter is the best from a design point of view. There are two general approaches to the solution: (1) the primary and secondary mirrors may both be hyperboloid surfaces of exact conic constants, and (2) fourth-order deformations from spherical surfaces may be used. Theory exists by which each form can be calculated, and computer programs exist to make the calculations required.

Numerous telescope systems have been designed and evaluated by NASA, and these have been almost entirely of the Ritchey-Chretien design class. Before this new method was evolved, the procedure used was: (1) trace two paraxial rays through spherical mirrors and determine the third-order aberrations of the system, (2) use the aberration data to determine a conic constant for the primary and for the secondary mirrors, and (3) use the conic constants and other system data to determine an optimum solution of conic surfaces.

The complete system for Ritchey-Chretien telescope design is illustrated in the figure. Steps 1 and 2 have been combined into one program called TELDESIN, which will design a Cassegrainian, a Dall-Kirkham, or a Ritchey-Chretien telescope system using third-order theory.

Referring to the flow chart, the steps followed in the new system are easily seen by the reader. The first-order optics, which determine focal length and f/number, are introduced as mirror radii, primary aperture, and intervertex distance into program TELDESIN. Program TELDESIN computes conic constants for the primary and secondary mirrors by third-order aberration theory. This constitutes Step 1.

Step 2. The conic constants and first-order optical parameters are introduced to program SPADE. By ray-tracing and computing rms spot sizes, program SPADE evaluates an error function which is then

automatically minimized by varying the conic constants of the mirrors. Typical values are slightly more than 1 for the primary, and slightly more than 2 for the secondary.

Step 3. The refined conic constants and the radii of curvature of the mirrors are introduced into program SAG, which computes the sagittal distance of the mirror surface from the vertex plane, as a function of distance from the optical axis.

Step 4. The table of sagittal distances is introduced into program CURVEFIT, which computes the coefficients of second-power and fourth-power terms in a polynomial expression for sagittal distance:

$$S = P_1 y^2 + P_2 y^4$$

Step 5. The two polynomial coefficients for each mirror are then introduced into program SPADE operating in the aconic mode. The coefficient P_1 is held constant, because it determines the first-order optical properties, and also because the secondary mirror typically obscures about one-half of the diameter of the primary mirror. By varying the coefficient P_2, performance is optimized, resulting in a fourth-order design. By varying P_3 a sixth-order design is obtained.

Step 6. The polynomial coefficients are then introduced into program SAG, to obtain a table of sagittal distances to aid in fabrication of the aconic surfaces.

Source: B. J. Howell of
Sperry Rand Corp.
under contract to
Goddard Space Flight Center
(GSC-11274)

Circle 4 on Reader Service Card.

MICROSCOPE/CAMERA ADJUSTABLE MOUNT

The fixture shown in the figures has been found to be a practical jig for providing swift and accurate positioning of a microscope and/or a camera in observing and photographing a test specimen at high magnification. This provides a stable platform for holding the microscope/camera and is adjustable in four directions: (1) up-down, (2) in-out, (3) left-right, and (4) rotational. After adjustments, it can be rigidly locked in the desired position.

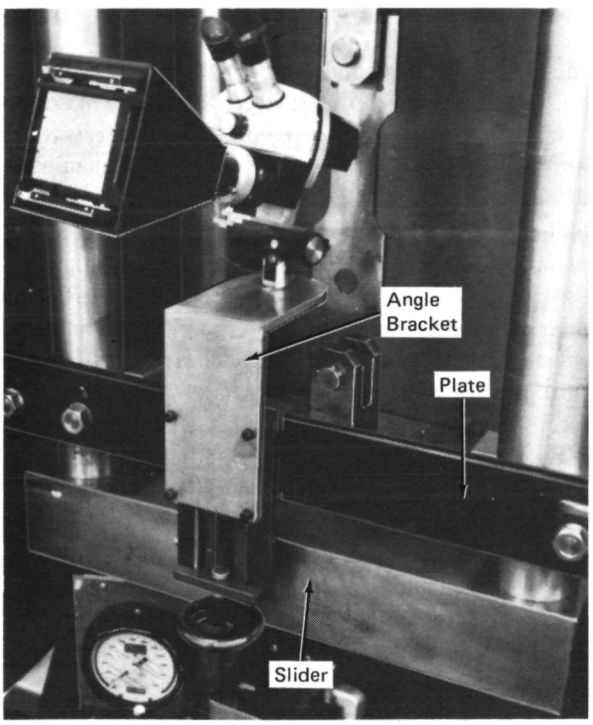

Mounted Camera

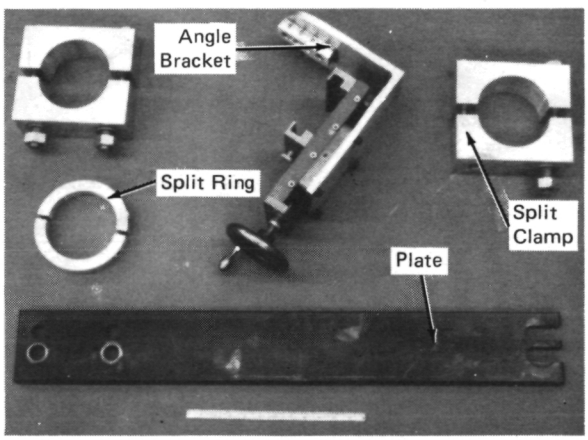

Parts for Mount

Source: R. J. Demonet of
Rockwell International Corp.
under contract to
Marshall Space Flight Center
(MFS-24027)

Circle 5 on Reader Service Card.

ACTIVE OPTICS CONCEPT USES A THIN DEFORMABLE MIRROR

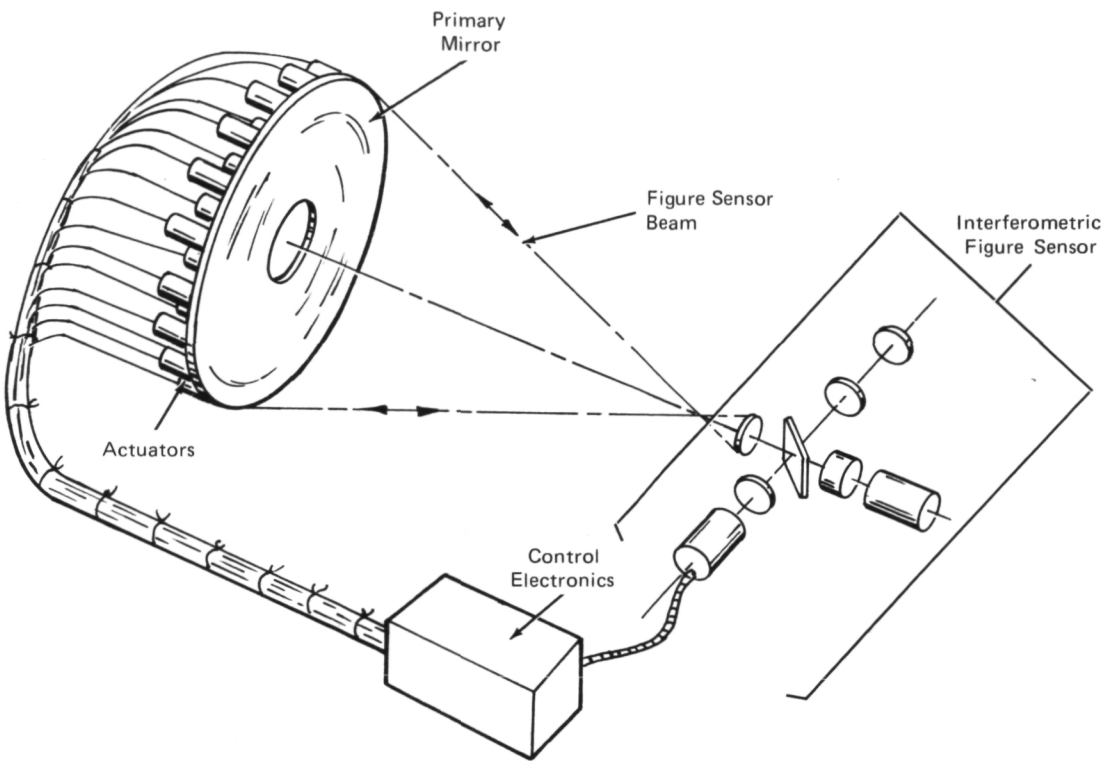

A NASA contractor has introduced a new concept for astronomical telescope construction, that utilizes a thin deformable primary mirror, which will produce an instrument capable of diffraction-limited performance for use in outer space research. The large booster capability developed for space exploration projects has made it possible to place large telescopes in orbit where they should be able to perform considerably better than ground-based telescopes, which are limited by atmospheric turbulence.

To take full advantage of the better seeing conditions above the atmosphere requires a telescope capable of diffraction-limited performance. The optical surfaces in such a telescope must be maintained to very close tolerances, and this is particularly difficult with respect to the primary mirror because of its size.

The active optics approach makes use of recent developments in interferometric figure sensing and servomechanical control techniques to provide a new procedure for obtaining the desired optical performance. The fundamental concept of active optics consists of measuring the surface shape (or figure) of a telescope primary mirror, computing the necessary electronic control signals, and physically aligning the mirror to its original design figure. The basic building blocks of the active system are shown in the illustration and include an interferometric figure sensor for detection of errors of the mirror surface figure, actuators to provide the precise mechanical displacement of the mirror surface required, and electronics for converting the errors observed by the figure sensor into controlling voltages and applying those voltages to the appropriate actuators to make error corrections. The initial experiment performed to demonstrate the feasibility of the concept consisted of measuring and correcting the alignment of individual elements of a segmented mirror. The specific objective of the experiment was to automatically align and maintain closed-loop control of a 0.5 m, three-segment mirror to within 1/20 wavelength rms of the design figure.

The experiment was very successful. Diffraction-limited performance was obtained, as proved by several independent optical tests. The composite figure of the segmented mirror assembly with closed-loop control was found to deviate from the design figure by less than 1/40 wavelength rms.

The following documentation may be obtained from:
National Technical Information Service
Springfield, Virginia 22151
Single document price $3.00
(or microfiche $2.25)

Reference:
NASA CR-1593 (N-70-33920) Development of an Active Optics Concept Using a Thin Deformable Mirror

Source: R. Crane, Jr., H. S. Hemstreet, C. La Fiandra, and H. J. Robertson of Perkin-Elmer Corp. under contract to Langley Research Center (LAR-10326)

APPLICATION OF SCANNING ELECTRON MICROSCOPE TO FRACTOGRAPHY

All fracture surfaces are inspected optically to orient the suspicious areas and to determine if artifacts are present on the fracture surface. The decision to use scanning electron microscopy (SEM) and/or transmission electron microscopy (TEM) for studying the suspicious areas must be based on several inherent requirements of either the specimen or the microscopy techniques available.

The SEM generally requires that the fractography sample have less than four square centimeters of surface and be less than four millimeters thick; whereas, TEM replicating techniques are not limited by sample size. Fractographic analyses by TEM require a minimum of three hours for sample preparation, while SEM sample preparation can be accomplished in ten minutes. Thus, direct observation of the sample in the SEM increases the volume of work capable of being performed daily while eliminating the possibility of introducing artifacts during replication for TEM. When SEM fractographic analyses are performed, the work must be completed before the sample can be relayed to other investigators, whereas, TEM replicas can be stored for future studies. Critical SEM failure analyses should be supported by TEM replication to protect against future inquiries. Rough fracture surfaces and composite materials having large abrupt topographical differences are usually difficult to replicate; however, since the SEM has a depth focus of 300 to 500 times that of the optical microscope, the entire field of view is always in focus. Observation of the fracture in the SEM can be varied from 20 diameters to 100,000 diameters with a probable peak resolution of 150Å, while the TEM can be varied between 1200 diameters and 150,000 diameters with a maximum resolution of 10Å.

The decision to utilize the SEM and/or the TEM for future analyses of fracture surfaces can be summarized by considering the following questions in order:

(1) Is the sample size prohibitive to SEM?
(2) Will sample trimming be detrimental to the analysis?
(3) How much time is available for analysis?

The majority of all metal or composite material failures can be examined by SEM if the specimens can conform to two restrictions which include: (1) the size of the sample must either conform to the sample limitations of the SEM being utilized or be trimmed to fit the SEM, and (2) the material must not vaporize under a low-accelerating potential electron beam or a vacuum environment. If the specimen cannot conform to these requirements, some form of replication must be attempted and a TEM utilized. Generally, the SEM provides a faster and cleaner method of performing fractographic analysis than a TEM; however, the SEM will not exclusively replace the TEM for versatility in applications other than surface topography studies.

Source: R. A. Parr, G. R. Marsh, and D. S. Kinkle, Jr.
Marshall Space Flight Center
(MFS-21411)

Circle 6 on Reader Service Card.

DIHEDRAL AZIMUTH REFERENCE: A CONCEPT

A space navigation technique has been proposed for obtaining a fixed azimuth direction to be used as a reference for a set of parallel azimuth planes. A reference direction is needed at each and every position which the theodolite may occupy on the vertical tooling bar.

The method originally conceived to provide this reference direction was a vertical line array of mirrors all made parallel to each other and mounted on a vertical fixed tooling bar. In use, whenever an azimuth reference was needed, the theodolite would be swung over to the mirror at the same height from the floor, and autocollimation was used to fix the azimuth reference. This reading would have to be corrected by a calibrated constant which related that particular member of the vertical mirror array to the one mirror in the array which was designated as the zero azimuth reference mirror.

The time consumed in maintaining the calibration of the vertical mirror bank was considered excessive, and a search was made for other methods which would not be so cumbersome and expensive, and make possible even more frequent calibrations and determinations of azimuth reference integrity at less cost and with higher accuracy. The multiple mirror array would have to be aligned by comparing two adjacent mirrors with a comparison autocollimator, then stepping up to the next mirror junction and comparing a third mirror with the second, and so on. This procedure would accumulate errors, and would not be subject to "closing" checks on these accumulated errors.

The solution to the problem is to replace the multiple array of azimuth reference mirrors with a single integral unit which performs the same function. There are three suggested approaches to the solution.

The simplest possible solution is a single mirror, rotatable about a horizontal fixed axis. A normal to this mirror surface would sweep out a plane which would be fixed in azimuth, and would be an azimuth reference direction. However, the mirror would have to be turned to a particular elevation position, so that the normal would intersect the elevation axis of the theodolite, so that the theodolite could be autocollimated on the mirror. This solution would then require a double "pointing" operation, and would be somewhat cumbersome to use.

The double pointing problem could be solved by spinning the mirror constantly. Readings would then be made in the short intervals of time during which the mirror normal was in the field of view of the theodolite, and theodolite elevation information would be lost due to blur. The elevation information is of no value in this instance, so this loss is no problem. The problem raised by this spinning mirror solution is one of signal-to-noise ratio. The signal-to-noise ratio is lowered by the duty cycle represented by the ratio of theodolite field-of-view to 360 degrees. This duty cycle problem could be solved by adding more mirrors to the rotating member, even a polygon. But here again, the solution presents more problems of complexity due to multiple mirrors, although a polygon would maintain its integrity better than the vertical mirror bank.

A position servo, driven by a readout of the elevation position of the theodolite, could control the position of the single azimuth reference mirror and automatically perform the double pointing function. This would be better than a spinning mirror or polygon, and would probably be used if there were not an elegant solution using optics.

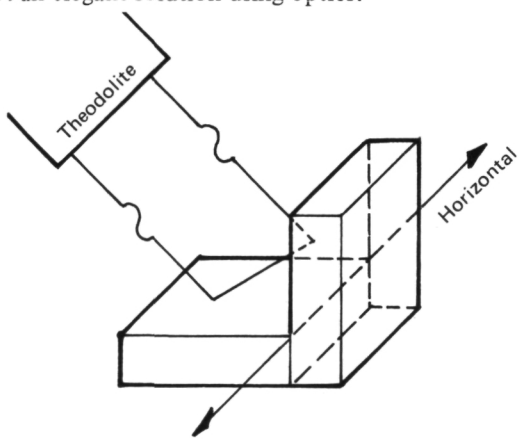

The optical solution is to have a type of mirror that will always reflect a ray of light back on itself, and which remains in a fixed position. Now this retroreflection must occur only when the incoming ray is in a certain plane, the azimuth reference plane (or a plane parallel to it). So a corner cube reflector would not serve the purpose, because it would destroy azimuth sensitivity. The answer is a dihedral reflector, or two mirrors at 90 degrees to each other, with the line of intersection in a horizontal plane and normal to the azimuth reference plane (see figure). This configuration will always redirect a ray anti-

parallel to itself, when the ray is in a plane normal to the line of intersection of the mirrors. If the ray is not in a plane normal to the intersection, the reflected ray will never be in a plane normal to the intersection. Thus we have a fixed dihedral, no moving parts, with full sensitivity in the desired direction (aximuth), and no sensitivity in the other direction (elevation).

Source: P. Seiler of
Sperry Gyroscope Co.
under contract to
Goddard Space Flight Center
(GSC-10301)

No further documentation is available.

SCAN MIRROR MOTOR ASSEMBLY

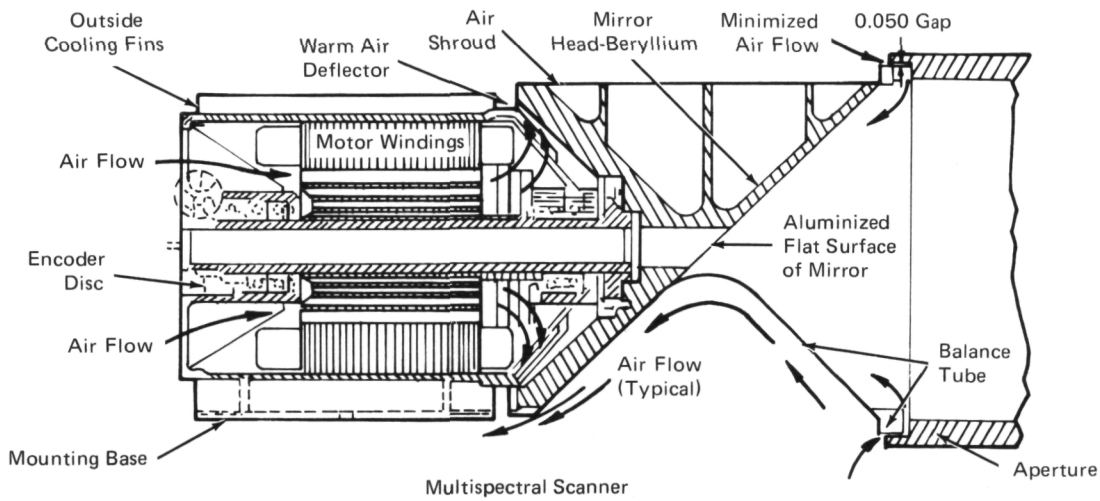

Multispectral Scanner

A new airborne multispectral scanner and data system instrument which incorporates some novel features is now being used by NASA (see figure). In this device a 22.9 cm mirror views the terrain and scans four calibration sources at speeds of up to 5500 rpm with only 20 arc-seconds of dynamic deviation. It is believed that this is the largest scan mirror ever to be operated successfully at such high speeds and with such low surface distortion.

The mirror used is flat, and it is attached directly to the shaft of a synchronous motor at an orientation of 45° to the motor spin axis. Beryllium was selected as the best material for the mirror substrate; reflectivity is provided by an electroless nickel plating, which is ground, polished, aluminized and protectively coated. A steel balancing ring on the light side of the mirror structure and outside the field of view was used to correct the imbalance of the mirror assembly. This counterbalance does not totally counteract the centrifugal forces involved, but at 5500 rpm the mirror deflections have a maximum deviation of 20 arc-seconds from the average surface slope.

The motor used is a 3 hp hysteresis synchronous motor which has low heat losses, high efficiency, and requires low power. Air drawn through the rear of the motor by a centrifugal fan on the motor shaft cools the assembly. A deflector on the front end cap prevents the warmed cooling air from contacting the mirror. Additional cooling is derived from fins on the motor housing, across which flows the air expelled from the heel of the mirror surface.

The development of the scan mirror motor assembly is a significant advance in the technology of instrumentation utilizing large scanning mirrors in high speed scanning operations. As such, it will be of interest to the optical community and users of optical and electromechanical scanning devices.

Source: W. Hamill of
Bendix Corp.
under contract to
Johnson Space Center
(MSC-13657)

Circle 7 on Reader Service Card.

A DYNAMIC MIRROR FLATNESS TEST

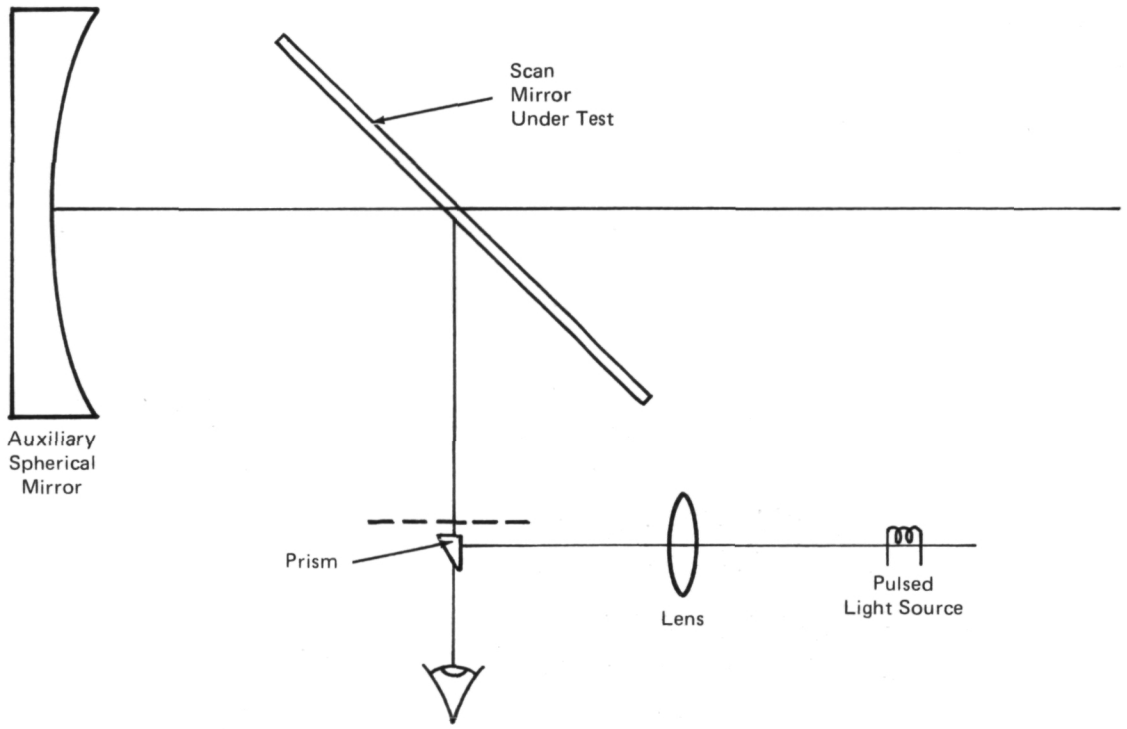

Optical Arrangement for Flatness Test

The illustration indicates an effective and easy method of measuring the change in figure (flatness) of a scanning mirror when the mirror is subjected to an external force of short duration. The test is performed with a Ronchi ruling at or near the center of curvature of an auxiliary spherical mirror. The difference between the fringe (shadow) pattern in static and dynamic mirror modes is a measure of the change in figure of the mirror under test. The advantage of this procedure is that the test is performed in a dynamic rather than a static mode.

The scan mirror for the Multispectral Scanner Program is a 22.9 by 35.6 cm ellipse that is driven by a mechanical impulse applied to the mirror each half cycle. Since this large mirror has a very stringent flatness requirement (the optical figure of the mirror) which must be maintained under the severe dynamic loading of the drive mechanism, it became necessary to test the figure under operating conditions. This was not previously possible, and the present test was devised. The various components are arranged as shown in the figure. With the scanning mirror in a static mode at the position to be tested, a continuous light source is used to adjust the Ronchi ruling to or near the center of curvature of the spherical mirror. The scanning mirror drive is actuated and the external force applied. If the external force is applied repetitively, the light source may be replaced with a pulsed source (e.g., a strobe light) synchronized with the scanning mirror. When the Ronchi ruling is placed at the center of curvature of the auxiliary spherical mirror, any fringes (shadows) observed during the dynamic test will be a direct visual indication of the change of figure of the mirror being tested.

From the number, position, and shape of the fringes, the slope error of the mirror may be calculated. This method requires only visual observation to obtain quantitative measure of the change in figure of the mirror. For a more accurate and more detailed determination of the figure change, the Ronchi ruling may be placed inside the center of curvature. This will provide several fringes in both the static and dynamic modes. Photographs of the fringe patterns in the two modes may be compared and differences produced to obtain a map of the mirror figure. The spatial frequency of the Ronchi ruling may be selected to give an appropriate number of fringes for observation.

The deviation of the mirror from a plane may be determined by applying the appropriate mathematical formula to the measurement of the change in fringe pattern between the dynamic and static modes of observation.

Source: R. K. Kimmel and G. E. Speake of
Hughes Aircraft Co.
under contract to
Goddard Space Flight Center
(GSC-11290)

Circle 8 on Reader Service Card.

BLACK MIRROR

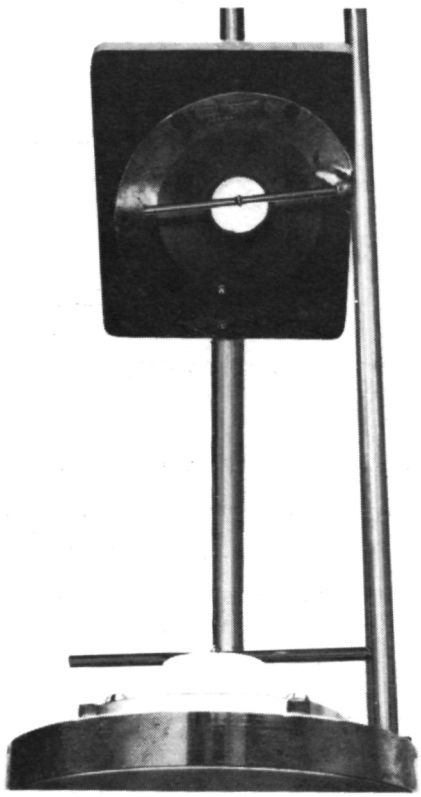

Plexiglas Black Mirror

A black mirror (see figure), constructed of Plexiglas and mounted above the furnace, facilitates problems associated with operations involving high temperature furnaces. The mirror is sprayed on one side with black paint and the side not sprayed reflects images. When properly prepared, this mirror reduces the glare by as much as 60 to 70 percent.

The installation of the mirror permits visual inspection of the furnace interior, permits visual inspection of test specimens inside the furnace, and serves as a visual aid in lowering specimens into the furnace and locating them afterwards. The black mirror can be an asset in any operation where a high-temperature (up to 2,273 K) brilliant light is present.

The mounted mirror allows both hands to be free and eliminates the need for wearing dark glasses. It also eliminates the necessity of climbing above the furnace and looking through smoked glass.

One such mirror installation has been in use for more than a year and a half. It was constructed from a section of Plexiglas measuring 1.27 x 11.4 x 15.2 centimeters.

Source: C. W. Whitehead
Langley Research Center
(LAR-10856)

No further documentation is available.

Section 2. Light Generation and Transmission

INTEGRATING SPHERE USED AS CONDENSER FOR OPTICAL SYSTEM

An integrating sphere (see figures) can be used as a condenser (light collecting device) for a photomultiplier tube (PMT). The sphere is capable of collecting light over a large scanning angle to accommodate a large film area. It provides a constant light input to the PMT, sufficient to maintain a satisfactory signal level.

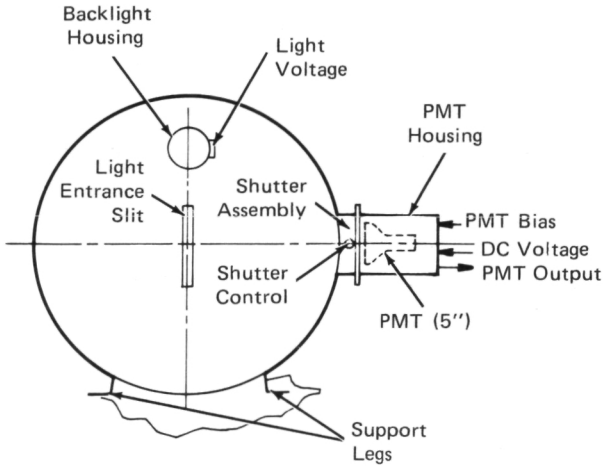

Figure 1. Integrating Sphere, Front View

The sphere is used in conjunction with a 19 cm radius glass platen (film plane), a rotating scanner having its axis located at a distance of 19 cm from the sphere, and laser optics. In operation, light enters the sphere by means of a narrow, adjustable slit near the film plane. The light contains diffuse and specular components as modulated by the film. A PMT housing is mounted at right angles to the plane of the scanning angle so that it collects light in accordance with the relationship:

$$E_{PMT} = E_{IN} \left[\frac{A_{PMT}}{A_S} \right] (e)$$

where: E_{IN} = Light energy input to system

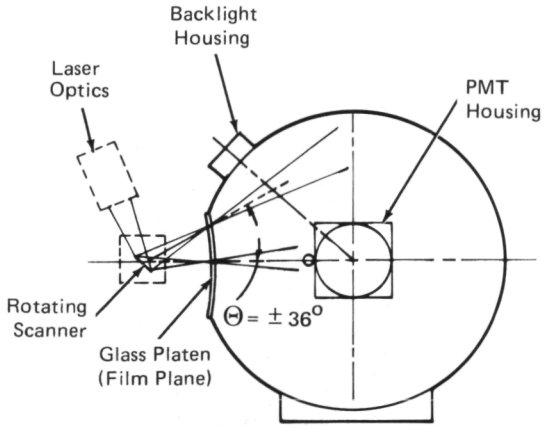

Figure 2. Integrating Sphere, Side View

E_{PMT} = Light energy input to PMT

A_{PMT} = Surface area of PMT photocathode

A_S = Surface area of integrating sphere

e = Light loss factor caused by absorption and loss of diffused light at slit and backlight.

Current methods are refracting components to image the exit pupil of the optical system onto the PMT. This technique is not effective over large scan angles. Also, the light energy impinging on the PMT relative to the scanning angle is not uniform, due to reflection losses and the aberration characteristics of refractive optics.

Source: J. C. Beck of
The Singer Co.
under contract to
Johnson Space Center
(MSC-14122)

Circle 9 on Reader Service Card.

HIGH EFFICIENCY OPTICAL BEAM SPLITTER DESIGNED FOR OPERATION IN THE INFRARED REGION

Optical beam splitters used in infrared spectrometers have been seriously limited by high absorption losses caused by the use of transparent thin metal films, and by a restricted spectral wavelength range and low efficiency due to the complexity of the multilayer thin-film design.

A three-phase program was undertaken to design, fabricate, and test a high efficiency beam splitter assembly which could operate in the infrared wavelength region between 5 and 30 μm.

Phase I was concerned with the selection of suitable substrate and coating materials for use as components of the beam splitter system. The optical and mechanical properties of five substrates were studied: potassium bromide (KBr), cesium iodide (CsI), thallium bromide (TlBr), calcium fluoride (CaF_2), and zinc selenide (ZnSe). Material homogeneity and optical transmission measurements were made and surface flatness tests were performed before and after temperature cycling.

After intensive investigation of each material, all but KBr and CaF_2 were eliminated as potential infrared beam splitter substrates suitable for vacuum coating and capable of maintaining performance after sustaining severe mechanical stress. KBr was found to satisfy the requirement for a substrate material capable of operating throughout the spectral region between 5 and 30 μm; CaF_2 proved suitable for narrowband applications. Potential beam splitter film designs were computed and curves predicting optical performance in the 5- to 30-μm range were obtained. A 13-layer film which yielded nearly equal broadband infrared reflectance and transmittance (and satisfied the mechanical requirements) was selected as the prototype beam splitter for fabrication.

The fabrication of the prototype beam splitter and compensating element was accomplished in Phase II. After fabrication, each element was tested for optical performance and mechanical stability.

The design, fabrication, and testing of prototype and production beam splitter mounts were completed in Phase III. Mounted beam splitters were tested in severe environmental conditions to determine their mechanical characteristics. The performance of the beam splitter during humidity tests indicated it could survive a 70% relative humidity for 24 hours at 30° C.

Source: P. L. Heinrich and R. C. Bastien of
Perkin-Elmer Corp.
under contract to
Goddard Space Flight Center
(GSC-10721)

Circle 10 on Reader Service Card.

HIGH QUALITY OPTICAL CHOPPER

A multi-layer, all-metal optical chopper has been developed that is superior in both mechanical and optical properties to those produced from photographic emulsions or by mechanical ruling. The new chopper pattern is free of organic compounds and has good adherence to the substrate.

Previous techniques produced extremely fragile patterns that were often damaged in cleaning and handling operations. The surfaces of choppers produced by photographic plates are covered with an organic emulsion that has poor light transmission qualities and cannot be used in the near ultraviolet region of the spectrum.

In the preparation of the new chopper, the first step involves the vacuum depositing of a multi-layer film on a quartz substrate. The film consists of chromium for adherence and silver for conductivity. Copper is then electrodeposited onto the silver and chemically blackened. The desired chopper pattern is next photoengraved using a modified version of the etched technique. A multi-bath operation completes the process.

The method described results in the production of a unique all-metal pattern (with superior adhering qualities) on a transparent substrate to be used as a light chopper for the wavelength from 1750 to 7500 Å. The method was developed originally as part of a star-tracker project.

Source: W. O. Smith, Jr., and A. Toft
Goddard Space Flight Center
(GSC-10507)

No further documentation is available.

MONOCHROMATOR/DEPOLARIZER

The optical assembly shown in the figure serves as a static depolarizer for a grating monochromator used in a satellite. The monochromator/depolarizer passes light of a moderately narrow band, resists radiation damage, and is rugged enough to withstand space flight. It is less than 10 mm long, has 1-nm gratings, and is designed for light with wavelengths between 250 and 350 nm. The optical assembly shown reduces the dependence of the grating monochromator output on the polarized state of incident light.

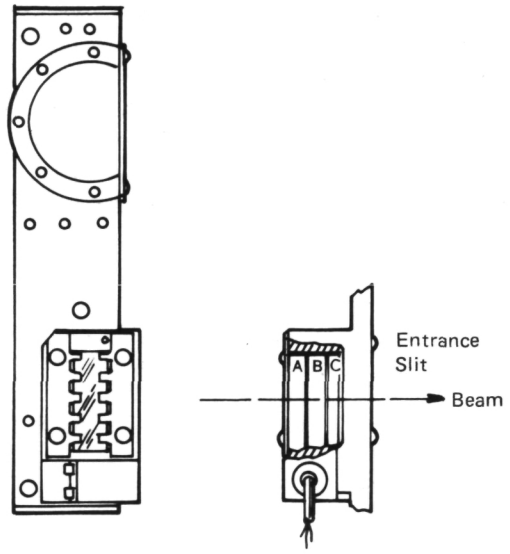

Assembly of Complete Depolarizer in a Backscatter Ultraviolet Instrument

The depolarizer consists of three optical components: a sapphire shield 5 mm thick and two calcite plates 3 and 6 mm thick, respectively. Orientation of the optical axis in all three of the parts is very important. The optical axis in the sapphire shield is oriented along the direction of propagation of the incoming beam into the instrument. The optical axis of the calcite plates is perpendicular to the incoming beam. The optical axis of the 3-mm plate is oriented at 45° to the slit height, in a plane parallel to the slit plane. The optical axis of the 6-mm plate is perpendicular to the slit height, in a plane parallel to the slit plane. The individual components are separated by Teflon gaskets, and two springs apply equal pressure along the longitudinal axis of the total assembly. The depolarizer assembly is positioned between the rotating circular shutter and the entrance slit and is mounted on the entrance-and-exit slit base plate.

The beam entering the instrument passes through the sapphire shield, the 6-mm calcite plate, and the 3-mm calcite plate, successively, before passing through the entrance slit. The depolarizer does not interfere with the field of view, f/ number, or energy to the monochromator; and it effectively reduces polarization sensitivity of the monochromator.

Source: W. A. Hanning of
Beckman Instruments, Inc.
under contract to
Goddard Space Flight Center
(GSC-11245)

Circle 11 on Reader Service Card.

LUMINESCENT SCREEN COMPOSITION

A luminescent screen composition has been developed upon which a photographically produced image is projected, usually from a transparency, by means of ultraviolet light. The composition includes a mixture of phosphors whose spectral emissions differ. When excited, the phosphors emit their characteristic color.

The luminescent composition for the faces of conventional cathode-ray tubes (CRT's) is deposited as selectively-positioned phosphor dots. This conventional arrangement of dots necessitates the use of an aperture mask and three electron guns. In the present invention, the composition is a mixture of nonlinear and linear phosphors. By substituting an overall smooth coating of this composition, the dot pattern, the shadow mask, and two of the three electron guns are eliminated. By varying the electron beam exciting current, different colors become visible. With the mixture of linear and nonlinear phosphors, red predominates at a current of 1 μA, and green predominates at a current of 10 μA. Many different hues result with intermediate electron beam currents. The figure illustrates apparatus employing this novel composition in a luminescent screen.

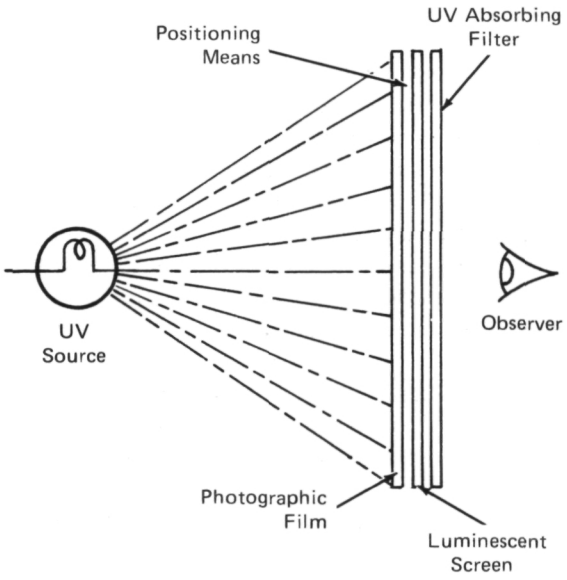

Use of this innovation permits the display of polychromatic luminescent images under extremely reliable conditions. Over the brightness range available with a monochromatic transparency, it is possible to differentiate between approximately ten brightness levels. However, when viewing a polychromatic image, it is possible for an observer to discriminate about 200 separate hues at a constant brightness level. Thus, image displays are available in different colors for better discrimination of objects being viewed. The simplicity of producing the multicolor display screen and its reliability represent important advances in the use of this apparatus.

Source: E. H. Hilborn
Electronics Research Center
(ERC-10010)

Circle 12 on Reader Service Card.

TUNGSTEN FILAMENT POINT LIGHT SOURCE

A tungsten filament configuration has been developed to supply an efficient point source of light. The advantages provided by this approach are: (1) a light source closely resembling a point is produced, (2) illumination is stable, and (3) the aperture is dimensionally stable.

The current method of producing a point source of light utilizes a miniature arc or a conventional incandescent lamp with an optical system. The miniature arc provides a point of light that is not small enough and is not dimensionally or photometrically stable. The conventional lamp plus optics is massive, expensive, and not efficient.

The new unit consists of a tungsten ribbon filament housed in an opaque container close to the filament. This arrangement produces a uniform cone of light over an extremely acute cone angle. Refinements would vary in slight details, such as electrode to inhibit darkening of window by evaporation, or the addition of iodine to enhance operation.

Source: R. Little of
AVCO Corp.
under contract to
Goddard Space Flight Center
(GSC-10868)

No further documentation is available.

CALIBRATION OF RADIOMETERS FOR HEMISPHERICAL INFRARED RADIATION IN VACUUM ENVIRONMENTS

A technique has been developed that provides a method of calibrating radiometer response to hemispheric (incident from all directions) blackbody radiation by measuring its signal in an evacuated cryogenic enclosure. In the requirements for space environment simulation, it is often necessary to measure infrared radiation in a vacuum. The infrared radiation measured in these circumstances is usually not of a point source nature, i.e., it approaches the surface of investigation from many directions. Therefore, a radiometer is needed for measuring which is calibrated for hemispherical conditions and which is calibrated for operation within a vacuum.

Currently, a radiometer is calibrated against a point light source in air and is then calibrated for air-to-vacuum sensitivity ratio. An approximation must then be made on the adjustment necessary for sensitivity to hemispherical radiation. Further, another approximation must be made to translate the calibration made with visible and near infrared light to sensitivity for middle and far infrared light.

It is possible to circumvent the latter approximations by placing the radiometer at one temperature and the cavity at another (higher) temperature; however, the air-to-vacuum sensitivity determination will still be necessary.

The radiometer is placed in a vacuum chamber equipped with cryogenically cooled black walls and evacuable to a pressure of less than 10^{-5} torr. The ratio of the distance between the radiometer and the chamber wall and the radiometer sensor diameter should be greater than 5. The radiometer temperature is maintained by water flow through the radiometer body and is monitored by a thermocouple welded or silver soldered to the water line within one inch (2.54 cm) of the radiometer body. The non-sensing portion of the radiometer is wrapped with a highly reflective substance, such as an aluminized polymer film. The chamber is evacuated and the walls cooled to stable conditions, at which time the radiometer output and temperature are recorded. The chamber wall temperature is also recorded. The radiometer sensitivity (calibration factor) is determined from the following relationship

$$S = \frac{\delta T_R^4 - \delta T_W^4}{V}$$

where S = radiometer sensitivity, heat per unit area per unit time

T_R, T_W = temperature of the radiometer and chamber wall, respectively

σ = Stefan-Boltzman constant (5.67×10^{-8} W/m^2 K^4).

The sensitivity determined is that for hemispherical radiation under vacuum conditions.

The technique provides a calibration factor for incident irradiance, being that the emittance and absorptance of the radiometer are the same in the infrared (assuming the radiometer surface is gray) as are many of the commonly used "black" coatings. Radiometer surface emittance is not necessary for the calibration because including it would give the sensitivity for absorbed irradiance, and to obtain incident irradiance data, the absorbed irradiance would have to be divided by the radiometer absorptance which for gray bodies is equal to the emittance, and thus cancels out the emittance term.

This technique is applicable to radiometers of the Schmidt-Boelter type; i.e., those that measure heat conducted through a slab the front and rear surfaces of which contain multiple thermocouple junctions, which measure and amplify the temperature differential across the slab thickness created by heat flowing through it. The slabs are mounted on blocks of relatively high thermal mass which are outfitted with conduits for water flow.

Source: C. M. Wolff of
Brown & Root-Northrop Laboratory
under contract to
Johnson Space Center
(MSC-14141)

No further documentation is available.

ATMOSPHERIC EFFECTS ON OPTICAL COMMUNICATIONS AND OPTICAL SYSTEMS

This item describes two separate investigations conducted under a NASA contract concerning the effects of atmospheric variations upon the behavior of light transmitted through the atmosphere. This work was administered under the technical direction of the Astrionics Laboratory of the Marshall Space Flight Center and the final report is now available.

The first study derives a theory for the angle of arrival fluctuations of a coherent optical beam propagated through the atmosphere. This investigation is primarily concerned with the tracking errors induced in radar by atmospheric turbulence. Expressions for the magnitude of atmospherically induced angle of arrival fluctuations have been derived from Tatarski's theory of the propagation of light through randomly inhomogeneous media.

The second investigation consists of the reduction and analysis of certain government-supplied data. These data concern the scintillation of a 10.6-μm laser beam and the signal-to-noise ratio in a frequency modulated CO_2 laser communications system. Techniques for reducing the subject data have been developed and software generated to implement the analysis on the IBM 360-50 computer. The results of the analysis are not complete at this time. However, preliminary results are available.

Source: W. E. Webb of
University of Alabama
under contract to
Marshall Space Flight Center
(MFS-20784)

Circle 13 on Reader Service Card.

Section 3. Laser Techniques

NOISE DIFFRACTION PATTERNS ELIMINATED IN COHERENT OPTICAL SYSTEMS

Noise diffraction patterns formed in the images of coherent optical systems can be eliminated by rotating the lenses about their optical axes. Such patterns, usually caused by dust or bubbles in or on the lenses, were previously reduced by carefully selecting the lens so that there was a minimum of bubbles and defects in the glass, and by keeping the lens surfaces extremely clean, even to the point of putting entire systems in vacuum. Neither of these methods, however, proved completely satisfactory, since any minute defect in the lens produced objectionable noise in coherent light, and the use of a vacuum system increased the cost and made working conditions more difficult.

With the lens rotation technique, the diffracted energy, normally concentrated over a very small area of the image, is spread over a much larger annular area. Unless the defect causing the diffraction lies very close to the optical axis, the diffracted energy is averaged out and can be ignored.

Specific advantages of the technique include a much simplified process of selecting the lenses to be used, reduced clean room requirements, and relatively low cost equipment requirements. In addition, the technique does not destroy the coherent filtering capabilities of the optical system.

Source: A. R. Shulman, G. R. Grebowsky,
H. B. Paull, and R. L. Hermann
Goddard Space Flight Center
(GSC-11133)

Circle 14 on Reader Service Card.

IMPROVED PUMP LAMPS

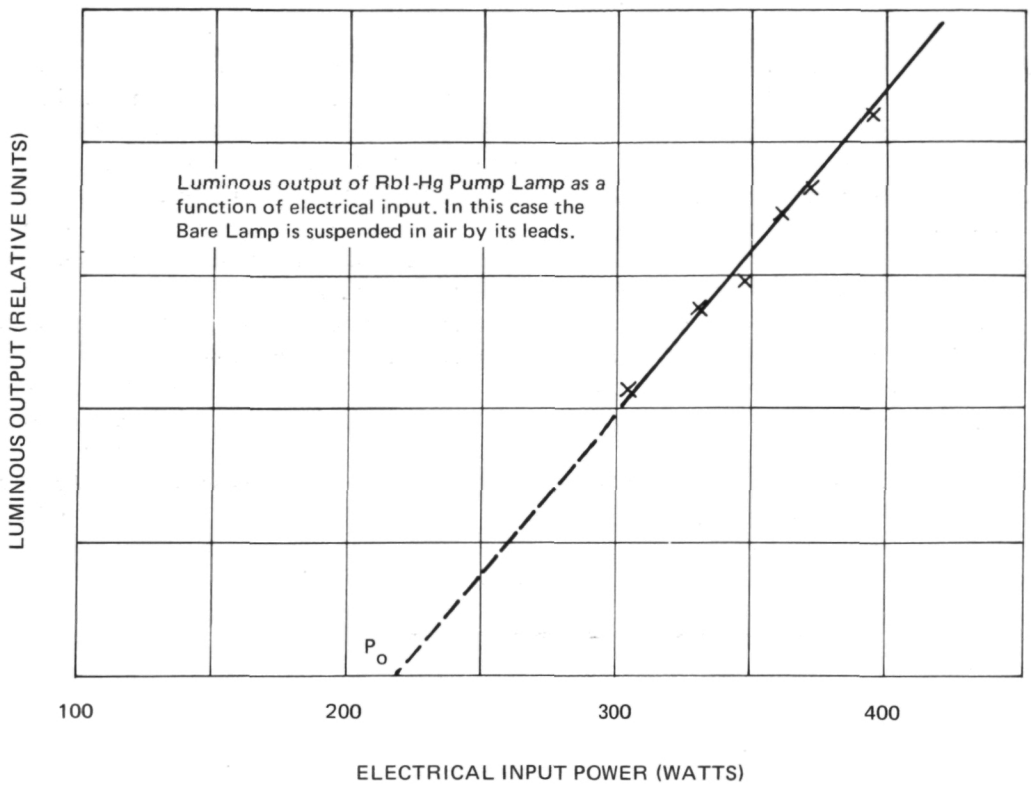

A technique for reducing the power requirements of rubidium iodine-mercury (RbI-Hg) flash lamps has been found to be practical. The power reduction is accomplished by insulating the flash lamp, i.e., enclosing the lamp body in an evacuated concentric quartz jacket. The vacuum separator provides thermal insulation, thereby reducing thermal losses and decreasing the amount of electric power needed for the lamp.

The figure shows the luminous power output as a function of electrical input power for a RbI-Hg lamp. The amount of electrical power necessary to reach linear threshold P_o is essentially wasted power, since it does not contribute to the optical pumping process when the lamp is placed in a laser. NASA has been interested in techniques to reduce this wasted power and thus increase the fractional amount of pump power that reaches the rod. The method used to reduce P_o is to isolate the lamp from its environment, thereby reducing the means by which energy can leave the lamp. Using one of the RbI-Hg pump lamps, P_o was experimentally determined for various degrees of insulation on the pump lamp, as follows:

The bare lamp is suspended in air; convective heat loss is very high (P_o = 230 watts).

A concentric quartz jacket is placed around the lamp and bonded to the lamp ends; convective heat loss is considerably reduced (P_o = 152 watts).

The concentric jacket is evacuated; convective losses are eliminated, but because jacket is bonded to lamp, there are conductive losses (P_o = 122 watts).

Source: Sylvania Electric Products, Inc.
under contract to
Marshall Space Flight Center
(MFS-21086)

Circle 15 on Reader Service Card.

A REAL TIME MOVING-SCENE HOLOGRAPHIC TECHNIQUE

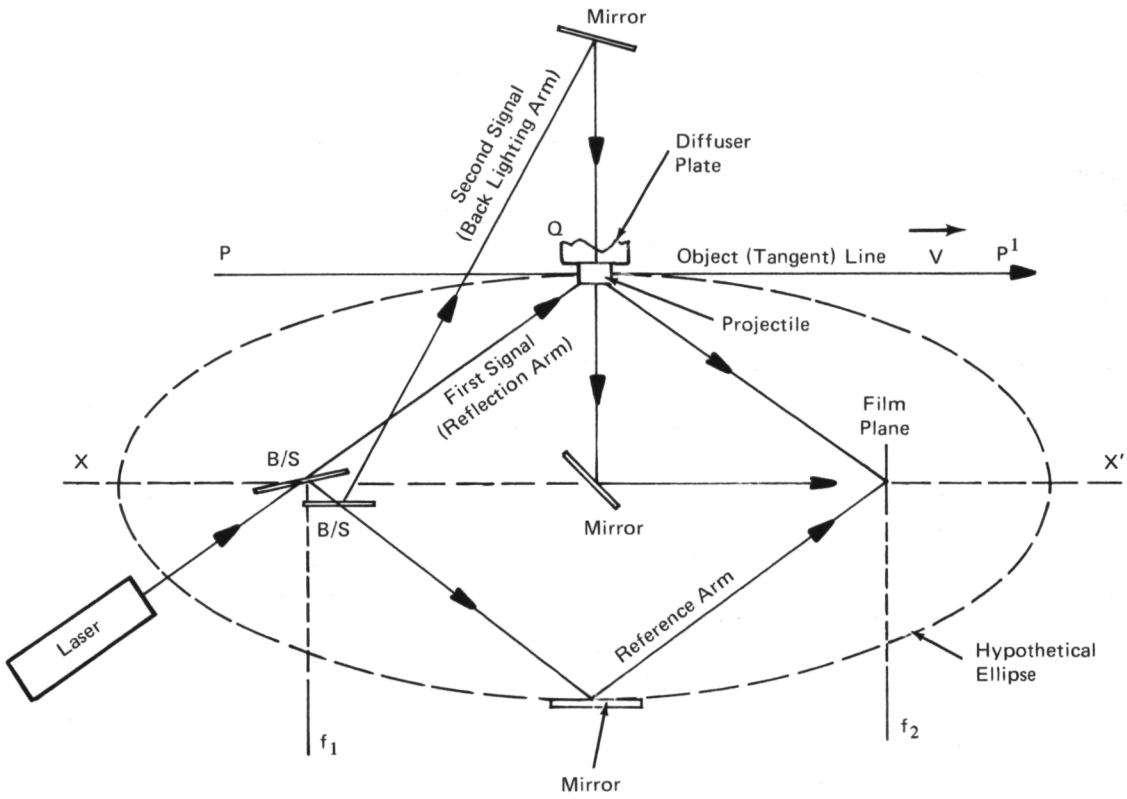

A novel technique for obtaining holographs of the front surfaces of objects moving at velocities of up to 9 x 10^5 cm/sec has been devised. The method can be a useful laboratory tool for the observation of rapidly moving objects, such as bullets, aerodynamic bodies, and bodies undergoing collisions or interaction. The process involves positioning the optical components of the holographic system so that the light paths from the laser source will be equal within the tolerances required for a hologram.

The specific orientation of the holographic system is based on the use of a hypothetical ellipse oriented with its major axis parallel to the "line of motion," defined by the moving projectile (see figure). This "line of motion" must be made tangent to the hypothetical ellipse at some point Q. One possible configuration of a holographic system positioned in this preferred orientation, inside the hypothetical ellipse, is shown in the figure. The specific orientation is defined by the following conditions: a thin film beam splitter (B/S) centered at the focus f_1 of the hypothetical ellipse; a film plane centered at the other focus f_2; and the major axis of this ellipse, defined by XX′ in the figure, being parallel to the tangent line, PP′ of the figure, which may be identified as the "line of motion" of the high speed projectile referred to above.

The exact matching of the length of the three arms is of no real concern if one has a source with sufficient coherence length. The source used in this experiment has a coherence length greater than three meters, operates at 6943 Å and has a pulse length as short as 15 nanoseconds. This system and orientation are presently being tested for the extreme velocities of the moving target, and the results will be published in the near future.

Source: R. L. Kurtz
Marshall Space Flight Center
(MFS-21087)

Circle 16 on Reader Service Card.

ORGANIC SCINTILLATING LASER

A high-power-density flashlamp is used to excite several new classes of aromatic hydrocarbons to laser thresholds. These compounds include organic scintillators used in particle detection. Flashlamp-pumped dye lasers have previously been limited to xanthene and coumarin derivatives. However, laser action has been observed from several other organic compounds when Q-switched high-power lasers are used as optical pumps.

In particular, the second harmonic of a Q-switched ruby laser has been used to pump secondary scintillators to laser thresholds. The secondary scintillators are commonly used as wavelength shifters, in order to match the photomultiplier response to the primary scintillator, in organic scintillator systems for nuclear and X-ray instrumentation. These secondary scintillabors exhibit a broad absorption spectrum in the near-ultraviolet region and have near-unity quantum efficiencies, large Stokes shifts, and short radiative lifetimes. Even with laser pumping, conversion efficiencies for the violet lasers are low, typically 5 percent which is poor compared to the visible and near-infrared dye lasers that show an order of magnitude higher efficiency.

Laser action has been observed from bis-POPOP, commercial solutions containing POPOP, and the blue dye acridone. A listing of the characteristics of the different laser materials has been prepared for reference purposes. Included are a few other scintillators that were readily available, but their thresholds for stimulated emission were not attainable with the present optical pump design. Laser emissions occurred in bands approximately 5 nm wide and, as expected, did not show the concentration-dependent spectral outputs, because of the large Stokes shifts associated with the materials.

The coaxial lamp laser system utilized a 0.2-pF cylindrical capacitor and a pressurized spark gap switch. The xenon-filled lamp had a 3.5-cm arc length, and the dye cell diameter was 8 mm. Rise time for the lamp was 100 ns. Plasma temperature in the lamp was approximately 35,000 K. The laser cavity had flat dielectric reflectors, and the dye cell had windows with antireflection coatings on the outside.

Although the lamp used in this system had excellent proportions, it was not specifically designed for ultraviolet pumping. A lamp of smaller cross section should increase plasma temperature and improve optical coupling efficiency by reducing end losses. With an improved lamp, more of the secondary scintillators, and even primary scintillators, should be able to reach laser threshold with flashlamp pumping.

Source: H. W. Furumoto and H. Ceccon
Electronics Research Center
(ERC-10282)

Circle 17 on Reader Service Card.

BALLOON-BORNE INSTRUMENT PACKAGE MEASURES VARIANCE OF LASER BEAM SCINTILLATION

A balloon-borne instrument package capable of measuring the variance of laser beam scintillation in the atmosphere has been developed. Evaluation of the design by NASA and participating scientific organizations has identified modifications which should insure the gathering of complete and meaningful data.

The equipment consists of a stabilized platform on which optical receivers are mounted along with the necessary communication links. The airborne package (see figure) has two detectors at each of two wavelengths (0.5 and 10.6 micrometers). One system operates with a fixed input mirror and the other system operates with a movable input mirror. In System I, the received beam is reflected off the fixed mirror onto the dichroic beam splitter. The beam splitter is used to separate the argon (0.5 μm) and the CO_2 (10.6 μm) beams. The dichroic beam splitter reflects the 10.6-μm beam through a refractive f/1 germanium lens and a germanium window onto an HgCdTe detector mounted on a liquid nitrogen dewar. The 0.5-μm beam passes through the dichroic beam splitter and is reflected off two mirrors and through an f/3 Galilean telescope lens arrangement with recollimates the 2.54-cm-diameter beam to a 1.5-cm-diameter beam onto the photomultiplier detector.

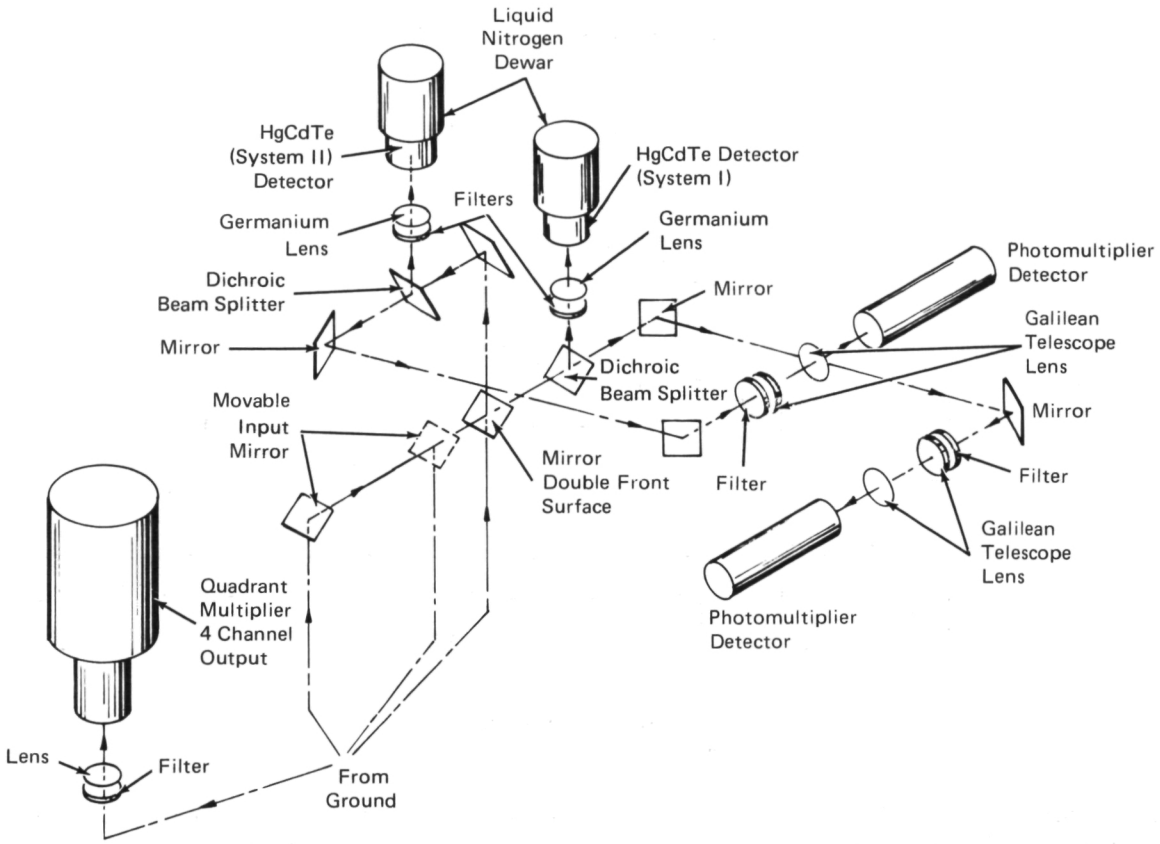

Optics for Balloon-Borne Laser Scintillation Detector

In System II, the received beam is reflected off the movable input mirror and two fixed mirrors prior to reaching the dichroic beam splitter. The optical arrangement for System II is identical to System I after the dichroic beam splitter. Additionally, located in the package is a quadrant multiplier four channel output with a 2.54-cm f/3 lens.

The electronic receiver package is designed to extract the atmospheric modulation on the laser beam and convert it to an analog signal of 1-kHz bandwidth. The laser beam is chopped with a 50% on-off duty cycle at the transmitter at a 5-kHz rate and transmitted through the atmosphere to the receiver, thus acquiring the modulation. The laser receiver observes both the chopped laser beam (with atmospheric modulation) and a slowly varying background. Since it is desirable to observe low level signals very accurately, it is necessary to eliminate effects of background. The chopped signal thus obtained can be reconstructed, using standard sampling techniques, and returned to the ground (transmitter bandwidth = 1 kHz).

Source: Sylvania Electric Products, Inc.
under contract to
Goddard Space Flight Center
(GSC-11186)

Circle 18 on Reader Service Card.

LASER VIBRATION ANALYZER

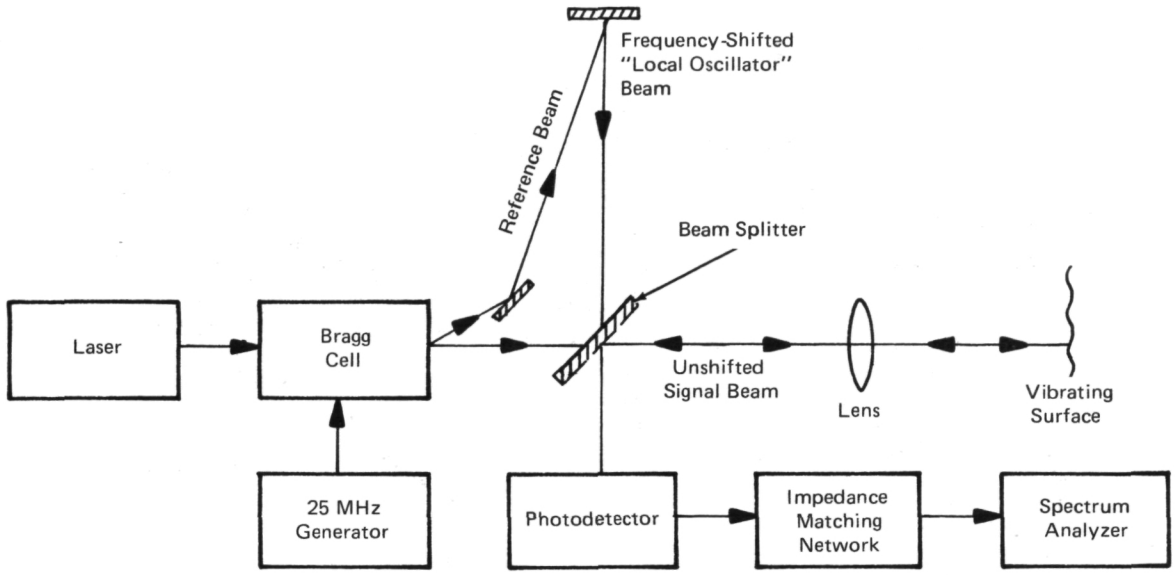

Block Diagram of Vibration Measurement System

The instrument system arrangement shown in the figure makes it possible to measure the vibration of a structure under test or in operation without attaching vibration sensors, such as strain gauges or inertial transducers.

The beam from the helium-neon laser is directed into a Bragg cell. One part passes directly to the vibrating surface; the diffracted portion passes to a beam-splitter mirror and directly into the photodetector to serve as the reference or local oscillator beam. The frequency of the diffracted laser beam is shifted in the Bragg cell by plane-traveling acoustic waves in water. The amount of the shift is large compared to the Doppler shifts in the light reflected from the vibrating surface. The reflected light from the vibrating surface returns through the instrument optical system to the beam splitter, where it is combined with the reference beam to produce interference with patterns which are sensed by the photodetector.

If the reflecting surface remains stationary, the interference patterns at the photodetector vary sinusoidally at the difference frequency, which is just equal to the shift or system intermediate frequency (I.F.). If the surface moves, the phase or frequency of the interference changes, producing frequency modulation of the system I.F. The shift provides a frequency bias so that motions toward or away from the instrument produce distinctive Doppler modulations which define the direction of the motion as well as its magnitude. The process signal from the detector is displayed visually on a spectrum analyzer.

Source: J. V. Foster
Ames Research Center
(XAC-01670)

Circle 19 on Reader Service Card.

DIFFUSION FILTER ELIMINATES FRINGE EFFECTS OF COHERENT LASER LIGHT SOURCE

The coherence property of a laser beam used as a photographic light source causes interference patterns which obscure details on the photographic film. A diffusion filter (see figure) comprised of small particles in colloidal suspension can be used to reduce the coherence of the laser beam. The intensity and collimation are moderately affected.

The size of the particles is selected to be larger than the wavelength of the laser beam, so that ordinary diffuse reflection from the surface of the particles will occur without degradation of the laser frequency. It is preferable to utilize a disperse phase of solid particles in a state of subdivision adapted to form a colloidal suspension in a liquid disperse medium. In a solid-liquid colloidal suspension, the fine particles remain suspended and will not readily settle out. Therefore, homogeneity without external mixing of the suspension is inherently achieved. Suitable colloidal-size suspensoids are prepared by suspending colloidal particles, such as milk solids or gold particles, in water.

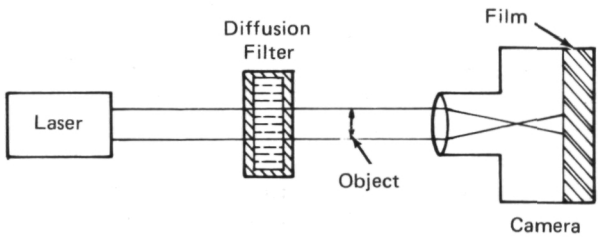

Use of Colloidal Diffusion Filter

Source: M. J. Olsasky of
Rockwell International Corp.
under contract to
NASA Pasadena Office
(NPO-10417)

Circle 20 on Reader Service Card.

SIMPLIFIED METHOD OF FRINGE MANIPULATION FOR HOLOGRAPHY

A simplified method for manipulating fringes in holographic interferometric testing has been developed (see figure). A hand-held, thin (1.6 mm), flat glass plate is inserted in the object beam as indicated. By tilting the mirror, the bull's-eye fringe pattern is moved about the object's surface. When the glass plate is removed, the fringe pattern is returned to the original position. The fringe pattern is not very sensitive to movement of the glass plate, so the mirror may be hand held and slowly manipulated over the surface. Since it is not necessary to touch the components on the table, no induced vibrations are created. Hence, the fringe pattern remains quite stable. This technique has been used for visual observation, but a light, easily movable holder could be added.

Previous methods of fringe manipulation involved microscrew adjustment of a mirror. These methods were slow, sensitive to hand vibrations, and difficult to return to the initial position. The new fringe manipulation technique overcomes these difficulties.

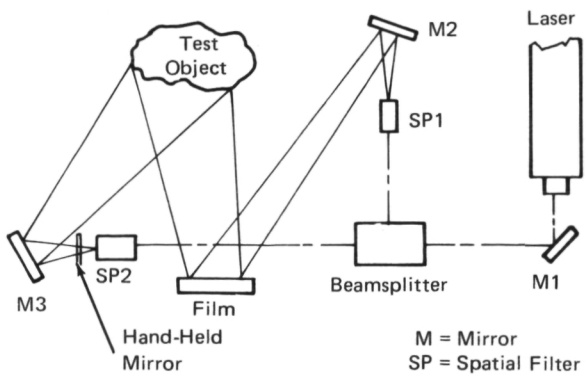

Holographic Interferometer

Source: F. H. Stuckenberg of
Rockwell International Corp.
under contract to
Johnson Space Center
(MSC-17922)

No further documentation is available.

STELLAR SPECTRUM CLASSIFIER

An apparatus has been designed to assist in classifying the spectra of stars photographed through an objective prism. With this apparatus, classification of the stars is made easier and more accurate. As shown in the figure, a photographic plate is placed in a holder which has an x-y coordinate readout to measure the relative positions of the spectra of stars on the plate. Collimated light from a laser passes through a spectrum on the plate, through a Fourier-transform lens, and then through an edge-coded film strip which contains complex-conjugate holograms of classified, representative stellar spectra. The film strip is moved until a hologram is reached which correlates with the Fourier transform of the spectral image. When this occurs, maximum energy passes through the hologram, through the inverse-transform lens, and into the video camera, causing a spot to appear on the monitor.

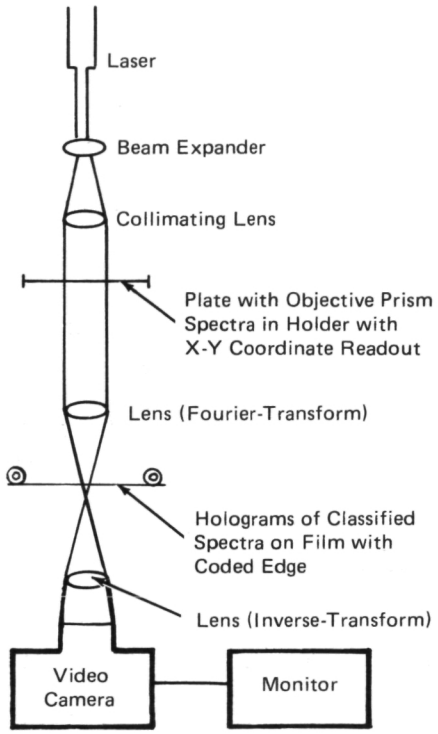

Classifier of Objective Prism Spectra of Stars

Used in conjunction with wide-field telescopes, stellar classification will be accelerated by the proposed system, since holograms are required only of the relatively few classified spectra, a small number in comparison to the large number of prints on file.

Source: J. H. Reid of
Lockheed Electronics Co.
Houston Aerospace Systems
under contract to
Johnson Space Center
(MSC-13450)

No further documentation is available.

Patent Information

The following innovations, described in this Compilation, have been patented or are being considered for patent action as indicated below:

Tungsten Filament Point Light Source (Page 15) GSC-10868.

This is the invention of a NASA employee, and U.S. Patent No. 3,549,886 has been issued to him. Inquiries concerning license for its commercial development may be addressed to the inventor: Mr. E. H. Hilborn, 32 Annese Road, Chelsea, Mass. 02150.

Laser Vibration Analyzer (Page 22) XAC-01670

This is the invention of a NASA employee, and U.S. Patent No. 3,355,934 has been issued to him. Inquiries concerning license for its commercial development may be addressed to the inventor: Mr. John V. Foster, Ames Research Center, Code P 200-18, Moffett Field, California 94035.

Diffusion Filter Eliminates Fringe Effects of Coherent Laser Light Source (Page 23) NPO-10417

This invention has been patented by NASA (U.S. Patent No. 3,587,424). Inquiries concerning nonexclusive or exclusive license for its commercial development should be addressed to:

Patent Counsel
NASA Pasadena Office
Mail Code I
4800 Oak Grove Drive
Pasadena, California 91103

NASA-Langley, 1976

NATIONAL AERONAUTICS AND SPACE ADMINISTRATION
WASHINGTON, D.C. 20546

OFFICIAL BUSINESS
PENALTY FOR PRIVATE USE $300

SPECIAL FOURTH-CLASS RATE
BOOK

POSTAGE AND FEES PAID
NATIONAL AERONAUTICS AND
SPACE ADMINISTRATION
451

U.S.MAIL

POSTMASTER: If Undeliverable (Section 158 Postal Manual) Do Not Return

"The aeronautical and space activities of the United States shall be conducted so as to contribute . . . to the expansion of human knowledge of phenomena in the atmosphere and space. The Administration shall provide for the widest practicable and appropriate dissemination of information concerning its activities and the results thereof."

— NATIONAL AERONAUTICS AND SPACE ACT OF 1958

NASA TECHNOLOGY UTILIZATION PUBLICATIONS

These describe science or technology derived from NASA's activities that may be of particular interest in commercial and other non-aerospace applications. Publications include:

TECH BRIEFS: Single-page descriptions of individual innovations, devices, methods, or concepts.

TECHNOLOGY SURVEYS: Selected surveys of NASA contributions to entire areas of technology.

OTHER TU PUBLICATIONS: These include handbooks, reports, conference proceedings, special studies, and selected bibliographies.

Details on the availability of these publications may be obtained from:

National Aeronautics and
Space Administration
Code KT
Washington, D.C. 20546

Technology Utilization publications are part of NASA's formal series of scientific and technical publications. Others include Technical Reports, Technical Notes, Technical Memorandums, Contractor Reports, Technical Translations, and Special Publications.

Details on their availability may be obtained from:

National Aeronautics and
Space Administration
Code KS
Washington, D.C. 20546

NATIONAL AERONAUTICS AND SPACE ADMINISTRATION
Washington, D.C. 20546